*Materials Science-Poland, 39(4), 2021, pp. 570-579*
*http://www.materialsscience.pwr.wroc.pl/*
*DOI: 10.2478/msp-2021-0045*

sciendo

# Delayed setting time for alkali-activated slag composites using activator containing $SiO_2$ and $Na_2O$

Chi-Che Hung[1], Wei-Ting Lin[2,*], Wei-Chung Yeih[3], Jiang-Jhy Chang[3]

[1]Institute of Nuclear Energy Research, Atomic Energy Council, Taoyuan 325, Taiwan
[2]Department of Civil Engineering, National Ilan University, Yilan 260, Taiwan
[3]Department of Harbor and River Engineering, National Taiwan Ocean University, Keelung 202, Taiwan

This study examines the influence of $SiO_2$ and $Na_2O$ mix proportions on the properties of alkali-activated slag (AAS) pastes. In order to solve the rapid setting problem associated with AAS, phosphoric or silicic acid is commonly added to the alkaline activator. The retarding effect of these additions suggests a close relationship between pH and setting time. In this study, AAS pastes with various $SiO_2$ and $Na_2O$ dosages were analyzed. Regression analysis was carried out using pH value and setting time to identify the main parameters affecting the setting time. Results showed that the alkali modulus (i.e., the weight ratio of $SiO_2$ over $Na_2O$) is correlated with the pH value. Specifically, the initial and final setting times were significantly reduced under lower $SiO_2$ and $Na_2O$ dosages. Therefore, a higher alkali modulus prolonged the setting time.

Keywords: *alkali-activated materials, setting time, silicate-based activator, microstructures*

## 1. Introduction

The first step in reducing global warming is to reduce $CO_2$ emissions. Green concrete makes use of industrial by-products to reduce the amount of aggregate as well as $CO_2$ emissions attributable to cement production [1]. Alkali-activated slag (AAS) is an innovative development in cement production aimed at achieving this goal [2]. AAS is a novel binder based entirely on slag with an activator [3], which leads to the production of a three-dimensional network of aluminosilicate materials [4], providing excellent mechanical properties [5] and durability [6]. In the reactive components of most AA binders, the availability of calcium for the production of a zeolite-like network structure is very low. Low-calcium fly ash and metakaolins are the most popular raw materials in the synthesis of AA binders [7]. Furthermore, the raw materials can be used without thermal treatment or calcination, which means that the energy requirements for manufacturing are far lower than those of Portland cement. In many cases, AAS can be used as a replacement for Portland cement to reduce $CO_2$ emissions [8].

Two extensive reviews have discussed the widespread application of AAS in Eastern Europe [9], Scandinavia, and China [10]. AAS composites (AASC) materials have recently been shown to outperform ordinary concrete based on Portland cement in terms of the former's low hydration heat [10], high early strength (>60 MPa) [11], and excellent durability in aggressive environments [12].

Nonetheless, one previous study has reported that this binder system is subject to a prohibitively short setting time (as short as 10 min) [13], under the accelerating effects of highly alkaline activators. AAS-based mixtures are also prone to cracking and premature failure as a result of excessive shrinkage under the effects of moisture loss [14], which can occur internally via hydration (autogenous shrinkage) [15] or externally via evaporation (drying shrinkage) [16]. The addition of suitable chemical additives [17] and alkaline activators to AAS-based mixtures has been reported to help improve the drying, setting time, and mechanical properties [18]. It has been suggested that increasing the concentration of $Na_2O$ can shorten the fi-

* E-mail: wtlin@niu.edu.tw

© 2021. This is an open access article distributed under the Creative Commons Attribution-NonCommercial-NoDerivatives 4.0 License.
(http://creativecommons.org/licenses/by-nc-nd/4.0/)

nal setting time of AASC [19]. Shi et al. [20] have shown that the alkali dosage and silicate modulus affected the alkali-silica reaction of AAS mortars, resulting in volumetric instability. AAS mortar also demonstrates excellent resistance to sulfate attack [21].

The strength development of AASC depends on the type and concentration of the activator [22]. Sodium silicate-based activators (i.e., sodium silicate plus sodium hydroxide) provide the best strength development performance; however, they are also associated with rapid setting times. This necessitates a stable high-pH environment [23] to prolong the reaction between raw material [24] and activator [25]. Phosphate [26] and malic acid [27] are often used to create this high-pH environment.

However, previous studies have found that pH may be one of the factors [10] affecting the setting time of AAS [27]. This study found that pH may not be the main factor affecting the setting time of AAS and that the amount and proportion of mixed alkaline activators have a significant effect on the setting time. Therefore, it has been deemed worthwhile to investigate the effect of $SiO_2$ and $Na_2O$ dosages on pH value and AAS setting time. This study investigated the alkali modulus ($SiO_2/Na_2O$) in binary alkaline activators containing sodium hydroxide and sodium silicate, as well as its effect on pH value, setting time, and microstructure, for use as a reference in developing AAS-based mix designs.

# 2. Experimental

## 2.1. Alkaline activator preparation

Alkaline activators are made up of water, sodium silicate, and sodium hydroxide. The content of $SiO_2$ and $Na_2O$ in a given alkaline activator mix design depends on the volume of alkaline activator. To determine the $SiO_2$: $Na_2O$ ratio, the sodium silicate solution was first weighed to determine the weight of $Na_2O$ and $H_2O$. These values were then used to calculate the amount of NaOH and $Na_2O$ required to equal the $Na_2O$ content in the alkaline activator mix. Finally, the weight of water (distillate water) consumed in the preparation of alkaline activator is equal to the weight of total water minus the weight of water in the sodium silicate solution. In cases where phosphoric acid is added, we deduct the weight of phosphoric acid from the weight of water consumed in the preparation of the alkaline activator.

The process of mixing water, sodium silicate, sodium hydroxide, and phosphoric acid must be implemented in a systematic manner. This process begins with the mixing of sodium silicate with water, to which is added sodium hydroxide under stirring until it dissolves entirely (including sediment). A reaction between sodium silicate and sodium hydroxide increases the temperature of the resulting solution. In the event that phosphoric acid is added to the solution, it is important to maintain stirring until all of the sediment (i.e., sodium ions and phosphoric acid) disappears. When the alkaline activator reaches room temperature, it is ready for use in the production of AAS.

## 2.2. Materials, mix design, and test methods

Solid sodium hydroxide (in the form of pellets), liquid sodium silicate, and pure water were used in the preparation of alkaline activators with various $SiO_2$ and $Na_2O$ ratios. The slag in the current study was ground granulated blast-furnace slag, the composition of which is listed in Table 1. The fineness of slag was 4,000 $cm^2/g$, and the grain size distribution of the slag is summarized in Table 2. The sodium hydroxide used in the experiments was of reagent grade, the chemical composition of which is shown in Table 3. The sodium silicate was extrapure reagent grade, the chemical composition of which is provided in Table 4.

In all AASC designs in this study, the liquid/binder ratio (i.e., the ratio of alkaline activator to slag by weight) was fixed at 0.5. The mix designs used in this study are listed in Table 5. In each series of experiments, the pH of the powder samples ground from the concrete specimens was measured in accordance with the specifications of the American Society for Testing and Materials (ASTM)-E70. Initial and final setting times were established using the Vicat test in accordance with ASTM

Table 1. Chemical and physical properties of slag

| | | |
|---|---|---|
| Main chemical composition of slag (by weight %) | $SiO_2$ | 33.87 |
| | $Al_2O_3$ | 14.42 |
| | $Fe_2O_3$ | 0.69 |
| | CaO | 39.54 |
| | MgO | 5.35 |
| | $SO_3$ | 2.47 |
| Basicity coefficient $K_b$ | (CaO+MgO)/($SiO_2$+$Al_2O_3$) | 0.93 |
| Physical properties | Specific weight | 2.90 |
| | Ignition loss (%) | 0.28 |

*Note*: Results of the author's analysis using X-ray fluorescence.

Table 2. Grain size distribution of the slag

| **Sieve size** | **No. 50** | **No. 100** | **No. 200** | **No. 325** | **Bottom** |
|---|---|---|---|---|---|
| Cumulative retained percentage (%) | 0.20 | 0.40 | 32.50 | 77.23 | 100.00 |

Table 3. Chemical composition of sodium hydroxide used in experiments

| **Chemical composition** | **Content (wt. %, maximum)** |
|---|---|
| Chloride (Cl) | 0.005 |
| Sulfate ($SO_4$) | 0.003 |
| Silicate ($SiO_2$) | 0.01 |
| Phosphate ($PO_4$) | 0.001 |
| Heavy metal (As, Pb) | 0.001 |
| Iron (Fe) | 0.0007 |
| Aluminum (Al) | 0.003 |
| Calcium (Ca) | 0.001 |
| Magnesium (Mg) | 0.0005 |
| Potassium (K) | 0.1 |
| Total nitrogen (N) | 0.001 |
| Arsenic (As) | 0.0002 |
| Sodium carbonate ($Na_2CO_3$) | 2.0 |
| Assay (NaOH) | 95.0 |

*Note*: Results were obtained from the supplier.

Table 4. Chemical composition of sodium silicate used in the experiments

| **Items** | **Results** |
|---|---|
| Water-insolubles (%) | 0.01 (max) |
| $SiO_2$ (%) | 37.0 |
| $Na_2O$ (%) | 17.7 |
| Mole ratio | 2.16 |
| Fe (%) | 0.02 (max) |

*Note*: Results were obtained from the supplier.

C191 specifications. Scanning electron microscopy (SEM) analysis was used to characterize representative samples measuring 1 mm × 1 mm × 1 mm, in accordance with ASTM C1723 specifications. The specimen was mixed and placed in a steel mold and left at room temperature for 24 h before unmolding. The AASC specimens were then cured in saturated lime water for 3 days and subjected to SEM. The specimens for SEM were cleaned and placed in an oven (105°C, 24 h), dried, and then removed to room temperature (approx. 5 h); next, they were placed in a vapor-plating apparatus for gold plating. The specimens were then vacuum-dried (120 s) to complete the preparation process.

# 3. Results and discussion

## 3.1. Properties of alkali-activated liquid

NaOH, $Na_2SiO_3$, and $H_2O$ were combined in various proportions to form the various activators. Note that using aqueous NaOH alone would likely

Table 5. Mix designs

| Activator (g/l) | | Weight % | | | |
|---|---|---|---|---|---|
| $SiO_2$ | $Na_2O$ | NaOH | $Na_2SiO_3$ | $H_2O$ | Slag |
| 60 | 60 | 0.013 | 0.054 | 0.266 | 0.667 |
| 60 | 80 | 0.022 | 0.054 | 0.257 | 0.667 |
| 60 | 100 | 0.031 | 0.054 | 0.249 | 0.667 |
| 60 | 120 | 0.039 | 0.054 | 0.240 | 0.667 |
| 80 | 60 | 0.009 | 0.072 | 0.252 | 0.667 |
| 80 | 80 | 0.018 | 0.072 | 0.243 | 0.667 |
| 80 | 100 | 0.027 | 0.072 | 0.235 | 0.667 |
| 80 | 120 | 0.035 | 0.072 | 0.226 | 0.667 |
| 100 | 60 | 0.005 | 0.090 | 0.238 | 0.667 |
| 100 | 80 | 0.014 | 0.090 | 0.229 | 0.667 |
| 100 | 100 | 0.022 | 0.090 | 0.221 | 0.667 |
| 100 | 120 | 0.031 | 0.090 | 0.212 | 0.667 |
| 120 | 60 | 0.001 | 0.108 | 0.224 | 0.667 |
| 120 | 80 | 0.010 | 0.108 | 0.216 | 0.667 |
| 120 | 100 | 0.018 | 0.108 | 0.207 | 0.667 |
| 120 | 120 | 0.027 | 0.108 | 0.198 | 0.667 |

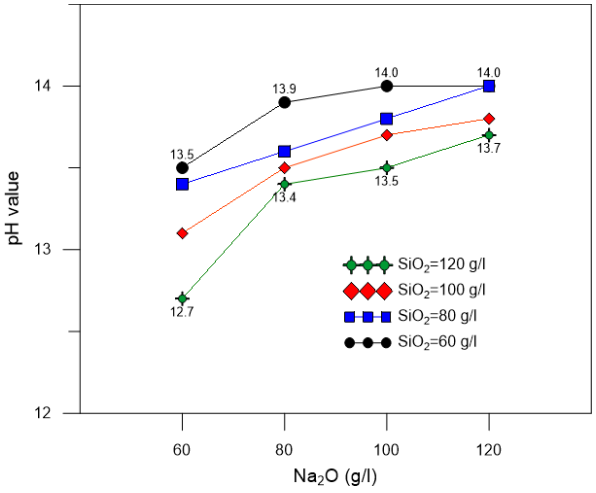



Fig. 1. pH value of activator as a function of $SiO_2$ concentration under various $Na_2O$ concentrations

result in excessively rapid setting. Hence, sodium silicate was added to the aqueous NaOH solution to retard this effect. Note that the addition of sodium silicate to highly alkaline NaOH lowered the pH. The silicate-based activator is a mixture of sodium hydroxide and sodium silicate; therefore, the production of $SiO_2$ can be traced back to $Na_2SiO_3$ (aq.), whereas the production of $Na_2O$ can be attributed mainly to NaOH (s.) with a small amount derived from $Na_2SiO_3$ (aq.). As shown in Figure 1, increasing the concentration of $SiO_2$ with a fixed concentration of $Na_2O$ reduced the pH value of the activator. Increasing the concentration of $Na_2O$ with a fixed concentration of $SiO_2$ increased the pH of the activator. This can be attributed to the fact that a higher concentration of $SiO_2$ resulted in the production of larger quantities of $SiO_3^{2-}$ capable of reacting with $H^+$ ions from the activator. Conversely, a higher concentration of $Na_2O$ made available a larger number of $Na^+$ ions to react with $OH^-$ ions from the activator.

The composition of alkaline activators can be characterized in terms of alkali modulus and total alkali content. Alkali modulus refers to the weight per unit volume of $SiO_2$ divided by the weight per unit volume of $Na_2O$ ($SiO_2/Na_2O$). Total alkali content refers to the total weight per unit volume of $SiO_2$ plus the total weight per unit volume of $Na_2O$ ($SiO_2$+$Na_2O$). As shown in Figure 2, increasing the dosage of $SiO_2$+$Na_2O$ produced a corresponding increase in the pH value when the alkali modulus ($SiO_2/Na_2O$) was fixed at 1.0. Increasing the dosage of $SiO_2$+$Na_2O$ increased the availability of both $SiO_2$ and $Na_2O$; however, the quantity of $OH^-$ (from $Na_2O$) exceeded the quantity of $H^+$ (from $SiO_2$), which caused the increase in pH. As shown in Figure 3, when the dosage of alkaline activator was fixed at 160 g/l or 200 g/l, the higher pH values were due to a lower relative proportion of $SiO_2$ or higher proportion of $Na_2O$. In other words, with the total quantity of $SiO_2$ and $Na_2O$ fixed, the higher pH values can be attributed to a lower alkali modulus.

As shown in Figure 4, increasing the alkali modulus led to a corresponding decrease in the pH value of the activator, i.e., pH values varied only with a change in the alkali modulus. Figure 5 illustrates the relationship between pH and $SiO_2$+$Na_2O$. The analysis of variations in pH under a fixed $SiO_2$+$Na_2O$ dosage indicates that the $SiO_2$+$Na_2O$ dosage had no effect on pH. The alkali modulus ($SiO_2/Na_2O$) can be used to indicate an increase in $SiO_2$ content, resulting in a lower pH.

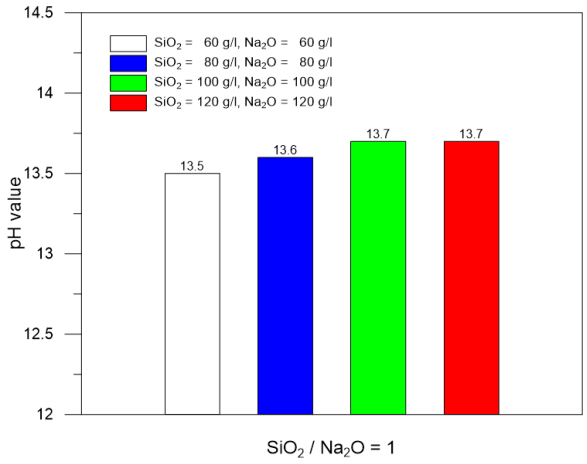



Fig. 2. pH values of activators with fixed alkali modulus of $SiO_2/Na_2O = 1$

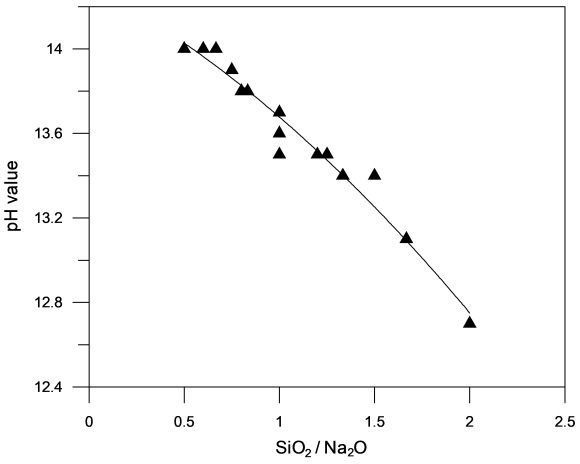



Fig. 4. Relationship between $SiO_2/Na_2O$ and pH value of activator

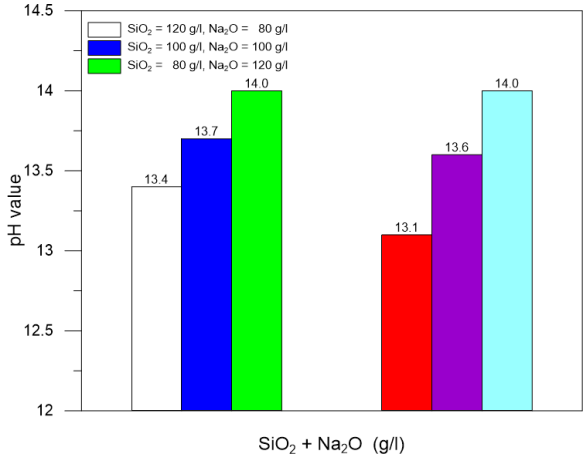



Fig. 3. pH values of activators with fixed total alkali content of $SiO_2$+$Na_2O$ = 160 g/l or 200 g/l

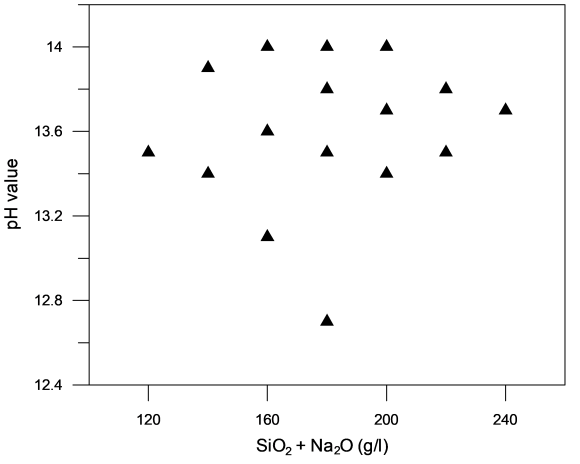



Fig. 5. Relationship between $SiO_2$+$Na_2O$ and the pH value of activator

This means that adding sodium silicate to a silicate-based activator (to retard the setting process) increases the alkali modulus ($SiO_2/Na_2O$) to above that of aqueous NaOH solution, while reducing the pH to below that of aqueous NaOH. Zhang's [28] study indicated that excessive $SiO_2$ content could hamper the alkali activation reaction and the excessive $SiO_2$ content decreases the overall pH, leading to a slower rate of reaction. The conclusion of the cited study is consistent with that of our study.

## 3.2. Setting time of AASC

The effects of $SiO_2$ and $Na_2O$ on the setting time were examined by varying their respective concentrations. As shown in Figure 6, increasing the concentration of $SiO_2$ under a fixed $Na_2O$ concentration reduced the setting time. It was due to the rapid production of the initial calcium silicate hydrate (C–S–H) gel as a result of the bonding of the calcium ions present in the slag to the silicate ions in the pore solution, which can harden the AASC paste. It is also consistent with the conclusions of the studies by Chang [29] study and Tong et al's [30]. At $SiO_2$ concentrations of 100 g/l or 120 g/l, increasing the concentration of $Na_2O$ decreased the initial and final setting times. However; the effect was insignificant at other $SiO_2$ concentrations.

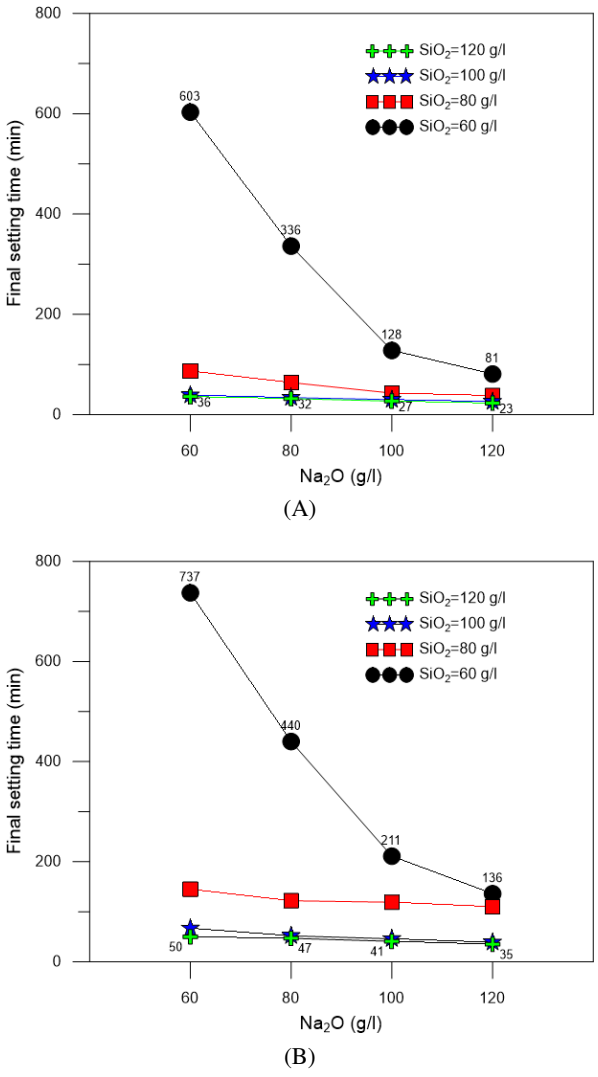



Fig. 6. Setting time ($Na_2O$ = 60–120 g/l): **(A)** initial time; **(B)** final time

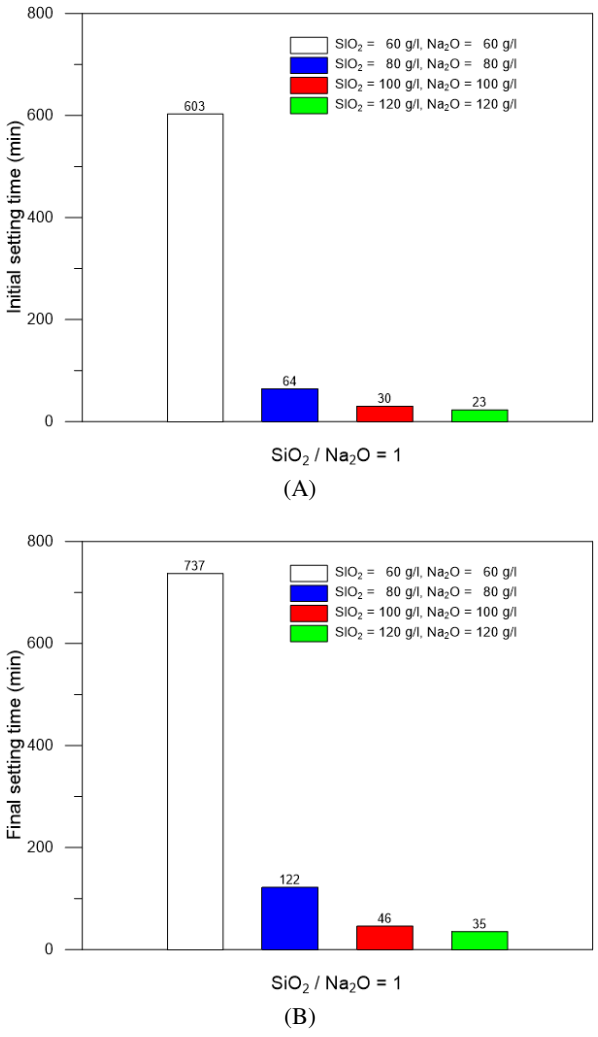



Fig. 7. Setting time under $SiO_2/Na_2O$ = 1: **(A)** initial time; **(B)** final time

Previous studies have demonstrated a correlation between the setting time of AAS pastes [29] and the concentration of $SiO_2$ and $Na_2O$ in the alkaline activator [30, 31]. It was then sought to determine whether the observed effect was the result of decreases in pH. Therefore, experiments were performed comparing the influence of alkali modulus ($SiO_2/Na_2O$) and total alkali content ($SiO_2$+$Na_2O$) on the setting time. Under a constant alkali modulus, increasing the $SiO_2$+$Na_2O$ dosage decreased the setting time (see Figure 7), while increasing the content of both sodium silicate and NaOH. It was observed that higher reactant concentrations produced higher reaction rates. Increasing the content of aqueous silica led to a higher $SiO_3^{2-}$ concentration, with a corresponding increase in the reaction rate. Increasing the NaOH concentration was also shown to increase the reaction rate, due to an increase in the $[OH^-]$ concentration, which facilitated the dissolution of $Ca^{2+}$ from the slag.

As shown in Figure 8, increasing the concentration of $SiO_2$ decreased the setting time, regardless of the $SiO_2$+$Na_2O$ dosage. In other words, a higher alkali modulus (indicating a larger quantity of $Na_2O$ dissolved from the sodium silicate) could be used as an index indicating a shorter set-

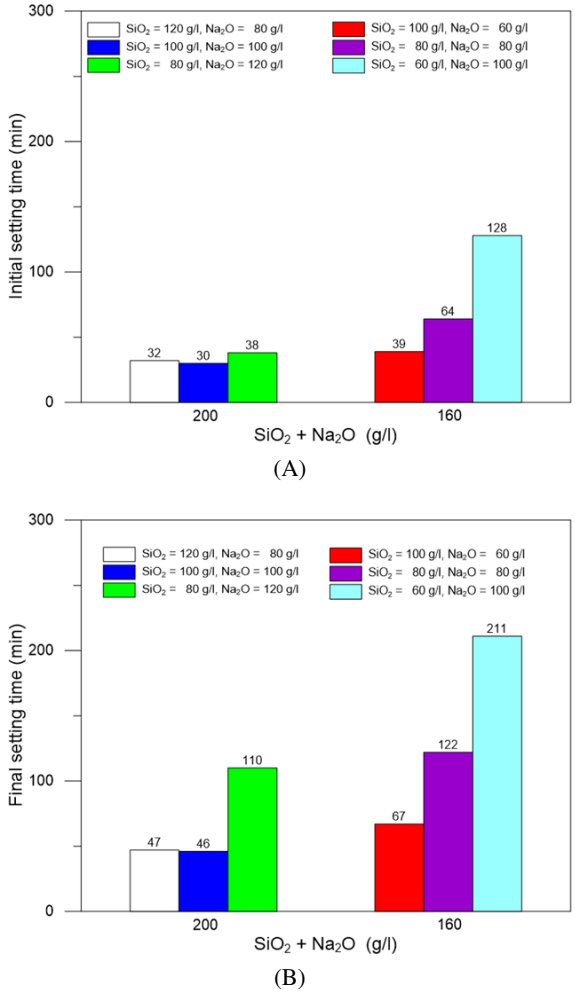



Fig. 8. Setting times under $SiO_2$+$Na_2O$ = 160 g/l or 200 g/l: **(A)** initial time; **(B)** final time

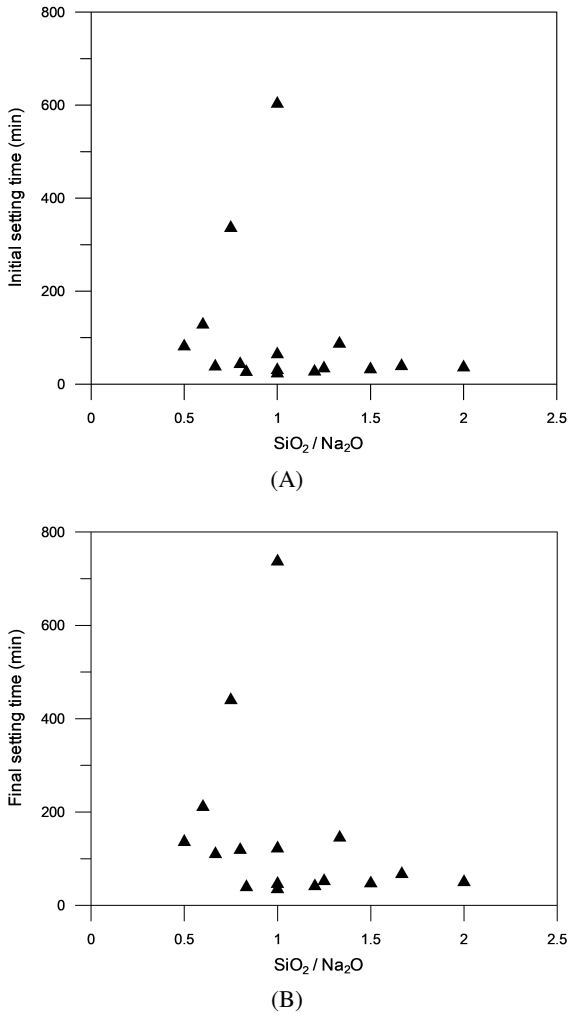
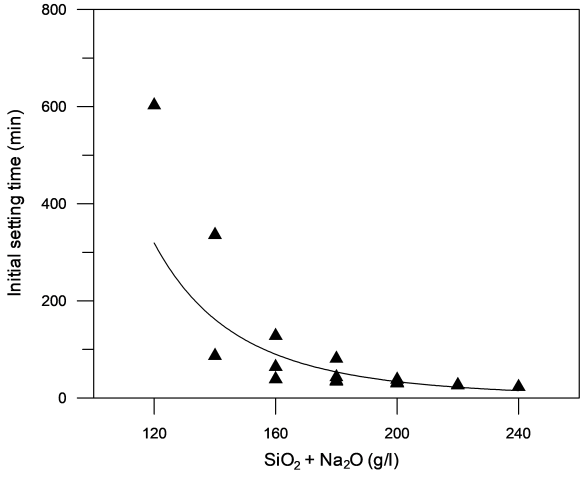



Fig. 9. Relationship between setting time and $SiO_2/Na_2O$: **(A)** initial time; **(B)** final time

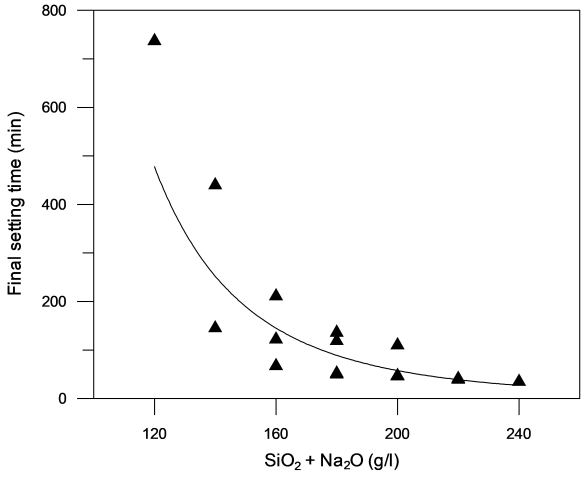
ting time. The results confirmed that NaOH facilitated the dissolution of $Ca^{2+}$ from slag particles; however, the content of aqueous silica also played a key role in the early hydration of AAS. From the results, it can be seen that the alkali content of $SiO_2$ had a significantly higher effect on the setting time than $Na_2O$. For a fixed total alkali content ($SiO_2$+$Na_2O$), the higher the $SiO_2$ content, the shorter was the setting time, which is in line with previous studies [29].

Regression analysis was used to compare the effects of alkali modulus ($SiO_2/Na_2O$) and total alkali content ($SiO_2$+$Na_2O$) on the setting time. As shown in Figure 9, there was a relationship between alkali modulus and setting time; however, a clear link was observed between alkali modulus and pH. From this, we can conclude that pH did not affect the initial or final setting time.

As shown in Figure 10, it was confirmed that $SiO_2$+$Na_2O$ dosage (i.e., the total concentrations of $SiO_2$ and $Na_2O$) had a pronounced effect on setting time, in a dose-dependent manner. This suggests that retardation of setting time cannot necessarily be attributed to a reduction in pH. The tests revealed that at $SiO_2$ = 60 g/l, the setting time retardation effects became evident under a high alkali modulus and became far more pronounced under a low alkali modulus. The effect of total alkali content on the setting time presented a clearer correlation.

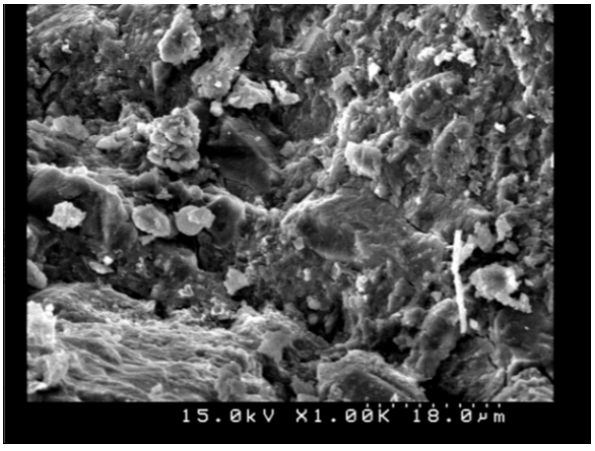



(A)

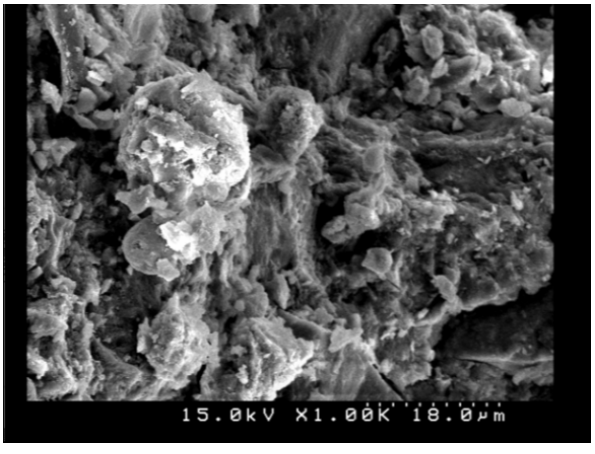



(B)

Fig. 10. Relationship between setting time and $SiO_2$+$Na_2O$: **(A)** initial time; **(B)** final time




(A)




(B)

Fig. 11. SEM photos (1,000× magnification): **(A)** $SiO_2$ = 120 g/l and $Na_2O$ = 120 g/l for 3 days; **(B)** $SiO_2$ = 80 g/l and $Na_2O$ = 80 g/l for 3 days. SEM, scanning electron microscopy

### 3.3. SEM analysis

SEM was used to examine the effects of $SiO_2$+$Na_2O$ dosage on the microstructure of AASC specimens. As shown in Figure 11, two specimens of the same alkali modulus presented a fine pore structure. Although the difference in pH values between the two specimens was not significant, the difference in $SiO_2$+$Na_2O$ dosage resulted in different microstructures. The differences in microstructure were mainly influenced by the setting time. SEM images obtained at 3 days revealed a large number of microfractures on the surface of the samples prepared using a paste containing 120 g/l of $SiO_2$ and 120 g/l of $Na_2O$. This can be attributed to the production of AAS amorphous reaction products under the effects of rapid hydration and condensation. These results support those of previous studies by Collins and Sanjayan [32], Yang et al. [33], and Opiso et al. [34]. By comparison, specimens prepared using paste containing 80 g/l of $SiO_2$ and 80 g/l of $Na_2O$ revealed totally and partially hydrated slag grains (due to a slow hydration reaction), as well as fewer microcracks. The main reaction products were fibrous structures corresponding to C–S–H gel, dense gel phase, partially reacted cenosphere, and a fully reacted matrix. A small quantity of calcium aluminosilicate

hydrate gel (C–A–S–H gel) was also observed.

The partially hydrated particles would continue to increase the strength of the paste as it was cured over time. Under the activator composition of $SiO_2/Na_2O$ = 1, the pastes set rapidly, but no visible cracks were observed on the microstructure surface. The faster setting time resulted in more partially hydrated slag grains on the surface of the specimens. The primary benefit of slowing the setting process through the addition of silicate-based activator is enhanced workability and the production of a complex microstructure with fewer cracks and more stable strength development. The results are consistent with previous studies by Atiş et al. [35] and Mastali et al. [36]. AAS has a more compact and dense crystal structure than the structure of C–S–H, formed during the hydration of ordinary Portland cement-based composites proposed by Alharbi et al. [37] and Paradiso et al. [38].

## 4. Conclusion

This study performed a systematic analysis of AAS paste and the effects of adding silicate-based activator. The results confirmed that the effect of silicic acid on setting time could be attributed to a decrease in the pH of the alkaline activator. Nonetheless, $SiO_2$+$Na_2O$ dosage had a more pronounced effect than the pH value. The results confirmed that the pH of the activator could be reduced by increasing the concentration of $SiO_2$ or $Na_2O$; however, the main factor affecting pH was actually the alkali modulus. Under a fixed liquid/slag ratio, the $SiO_2$+$Na_2O$ dosage and alkali modulus were both shown to affect the setting time. Under similar pH conditions, the pH value for $SiO_2$ = 120 g/l and $Na_2O$ = 120 g/l was 13.7 and the final setting time was 35 min; the pH value for $SiO_2$ = 80 g/l and $Na_2O$ = 80 g/l was 13.6 and the final setting time was 122 min. This showed that $SiO_2$+$Na_2O$ dosage was strongly correlated with setting time, whereas the alkali modulus was not.

## References

[1] Kamath M, Prashant S, Kumar M. Microcharacterisation of alkali activated paste with fly ash-GGBS-metakaolin binder system with ambient setting characteristics. Constr Build Mater. 2021;277:122323.

[2] Zhang B, Zhu H, Cheng Y, Huseien GF, Shah KW. Shrinkage mechanisms and shrinkage-mitigating strategies of alkali-activated slag composites: a critical review. Constr Build Mater. 2022;318:125993.

[3] Korniejenko K, Frączek E, Pytlak E, Adamski M. Mechanical properties of geopolymer composites reinforced with natural fibers. Procedia Eng. 2016;151:388–93.

[4] Saha S, Rajasekaran C. Mechanical properties of recycled aggregate concrete produced with Portland pozzolana cement. Adv Concr Constr. 2016;4(1):27–35.

[5] Solanki P, Dasha B. Mechanical properties of concrete containing recycled materials. Adv Concr Constr. 2016;4(3):207–20.

[6] Korniejenko K, Łach M, Mikuła J. Mechanical properties of raffia fibres reinforced geopolymer composite. In: Fangueiro R., Rana S, editors. Advances in natural fibre composites. Cham: Springer; 2018. pp. 135–144.

[7] Chen K, Lin WT, Liu W. Microstructures and mechanical properties of sodium-silicate-activated slag/cofired fly ash cementless composites. J Clean Prod. 2020;277:124025.

[8] Hafez H, Kassim D, Kurda R, Silva RV, Brito J. Assessing the sustainability potential of alkali-activated concrete from electric arc furnace slag using the $ECO_2$ framework. Constr Build Mater. 2021;281:122559.

[9] Roy DM. Alkali activated cements: opportunities and challenges. Cem Concr Res. 1999;29(2):249–54.

[10] Amer I, Kohail M, El-Feky MS, Rashad A, Khalaf MA. A review on alkali-activated slag concrete. Ain Shams Eng J. 2021;12(2):1475–99.

[11] Awoyera P, Adesina A. A critical review on application of alkali activated slag as a sustainable composite binder. Case Stud Constr Mater. 2019;11:e00268.

[12] Ho HL, Huang R, Hwang LC, Lin WT, Hsu HM. Waste-based pervious concrete for climate-resilient pavements. Materials. 2018;11:900.

[13] Gong C, Yang N. Effect of phosphate on the hydration of alkaliactivated red mud-slag cementitious material. Cem Concr Res. 2000;30(7):1013–16.

[14] Collins F, Sanjayan JG. Effect of pore size distribution on drying shrinkage properties of alkali-activated slag concrete. Cem Concr Res. 2000;30(9):1401–06.

[15] Parveen P, Singhala D. Development of mix design method for geopolymer concrete. Adv Concrete Constr. 2017;5(4):377–90.

[16] Jiang D, Li X, Lv Y, Li C, Jiang W, Liu Z, et al. Autogenous shrinkage and hydration property of alkali activated slag pastes containing superabsorbent polymer. Cem Concr Res. 2021;149:106581.

[17] Zhang B, Zhu H, Feng P, Zhang P. A review on shrinkage-reducing methods and mechanisms of alkali-activated/geopolymer systems: effects of chemical additives. J Build Eng. 2022;49:104056.

[18] Dener M, Karatas M, Mohabbi M. High temperature re-

sistance of self compacting alkali activated slag/portland cement composite using lightweight aggregate. Constr Build Mater. 2021;290:123250.

[19] Allahverdi A, Najafi Kani E, Esmaeilpoor S. Effects of silica modulus and alkali concentration on activation of blast-furnace slag. Iran J Mater Sci Eng. 2008;5(2):32–5.

[20] Shi Z, Shi C, Wan S, Zhang Z. Effects of alkali dosage and silicate modulus on alkali-silica reaction in alkali-activated slag mortars. Cem Concr Res. 2018;111:104–15.

[21] Dener M, Karatas M, Mohabbi M. Sulfate resistance of alkali-activated slag/Portland cement mortar produced with lightweight pumice aggregate. Constr Build Mater. 2021;304:124671.

[22] Caijun S. Strength, pore structure and permeability of alkali activated slag mortars. Cem Concr Res. 1996;26(12):1789–99.

[23] Pavel K, Oleg P, Hryhorii V, Serhii L. The development of alkali-activated cement mixtures for fast rehabilitation and strengthening of concrete structures. Procedia Eng. 2017;195:142–6.

[24] Gao X, Yu QL, Brouwers HJH. Apply 29Si, 27Al MAS NMR and selective dissolution in identifying the reaction degree of alkali activated slag-fly ash composites. Ceram Int. 2017;43(15):12408–19.

[25] Gao X, Yu QL, Lazaro A, Brouwers HJH. Investigation on a green olivine nano-silica source based activator in alkali activated slag-fly ash blends: reaction kinetics, gel structure and carbon footprint. Cem Concr Res. 2017;100:129–139.

[26] Fernandez-Jimenez A, Palomob JG, Puertas F. Alkali-activated slag mortars mechanical strength behaviour. Cem Concr Res. 1999;29(8):1313–21.

[27] Brough AR, Holloway M, Sykes J, Atkinson A. Sodium silicatebased alkali-activator slag mortars, part II. The retarding effect of additions of sodium chloride or malic acid. Cem Concr Res. 2000;30(9):1375–9.

[28] Zhang J, Ma Y, Zheng J, Hu J, Fu J, Zhang Z, et al. Chloride diffusion in alkali-activated fly ash/slag concretes: role of slag content, water/binder ratio, alkali content and sand-aggregate ratio. Constr Build Mater. 2020;261:119940.

[29] Chang JJ. A study on the setting characteristics of sodium silicate-activated slag pastes. Cem Concr Res. 2003;33(7):1005–11.

[30] Tong S, Yuqi Z, Qiang W. Recent advances in chemical admixtures for improving the workability of alkali-activated slag-based material systems. Constr Build Mater. 2021;272:121647.

[31] Choi S, Lee KM. Influence of $Na_2O$ content and Ms ($SiO_2/Na_2O$) of alkaline activator on workability and setting of alkali-activated slag paste. Materials. 2019;12(13):2072.

[32] Collins F, Sanjayan JG. Microcracking and strength development of alkali activated slag concrete. Cem Concr Compos. 2001;23(4–5):345–52.

[33] Yang LY, Jia ZJ, Zhang YM, Dai JG. Effects of nano-TiO2 on strength, shrinkage and microstructure of alkali activated slag pastes. Cem Concr Compos. 2015;57:1–7.

[34] Opiso EM, Sato T, Otake T. Microstructural properties of hardened cement paste blended with coal fly ash, sugar mill lime sludge and rice hull ash. Adv Concr Constr. 2017;5(3):289–301.

[35] Atiş CD, Bilim C, Çelik Ö, Karahan O. Influence of activator on the strength and drying shrinkage of alkali-activated slag mortar. Constr Build Mater. 2009;23(1):548–55.

[36] Mastali M, Kinnunen P, Dalvand A, Firouz RM, Illikainen M. Drying shrinkage in alkali-activated binders – a critical review. Constr Build Mater. 2018;190:533–50.

[37] Alharbi N, Varela B, Hailstone R. Alkali-activated slag characterization by scanning electron microscopy, X-ray microanalysis and nuclear magnetic resonance spectroscopy. Mater Charact. 2020;168:110504.

[38] Paradiso P, Santos RL, Horta RB, Lopes JNC, Ferreira PJ, Colaço R. Formation of nanocrystalline tobermorite in calcium silicate binders with low C/S ratio. Acta Mater. 2018;152:7–15.

*Received 2022-01-07*
*Accepted 2022-03-06*